

The inherent potential energy surface (IPES) and crystallization in water at deeply supercooled conditions

Fausto Martelli¹ Biswajit Santra¹ Robert A. DiStasio Jr.^{1,*} Roberto Car¹

¹Department of Chemistry, Princeton University, Princeton, NJ 08544, USA

*Present address: Department of Chemistry and Chemical Biology, Cornell University, Ithaca, NY 14853 USA



The IPES of water at standard density and pressure

- ▶ IPES¹: collection of local potential energy minima along an MD trajectory. By removing thermal excitations it allows to focus on structural effects.
- ▶ The local structure index I^2 is an order parameter that identifies low and high density local environments.
- ▶ The I distribution in the IPES is bimodal. Sites with $I > I_{min}$ are low density, sites with $I < I_{min}$ are high density.
- ▶ Clustering of sites of low and high I is observed in the IPES.

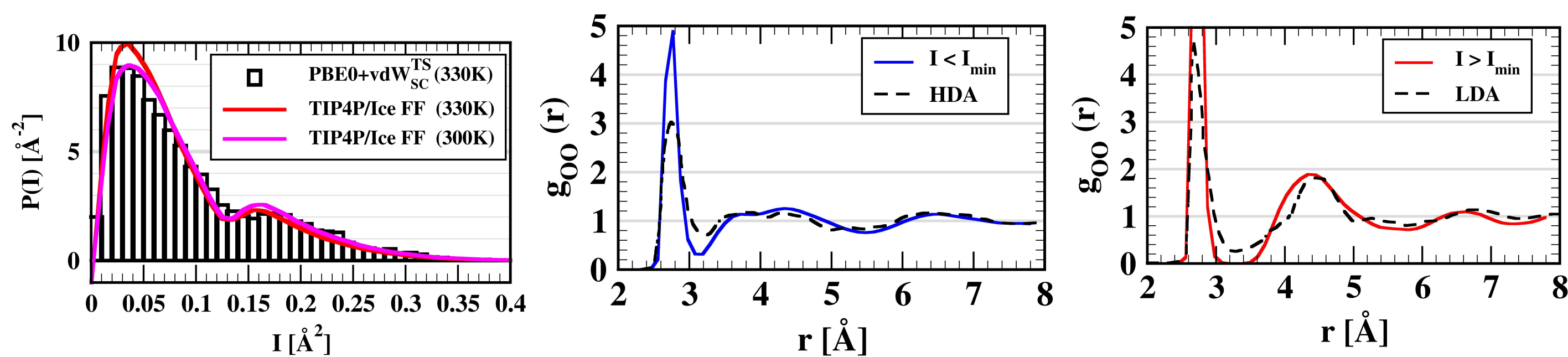


Figure 1 : Left panel: I distribution in the IPES from *ab initio* and model potentials. Middle panel: $g_{OO}(r)$ for low I sites compared to experimental $g_{OO}(r)$ of high density amorphous (HDA) ice. Right panel: $g_{OO}(r)$ for high I sites compared to the experimental $g_{OO}(r)$ of low density amorphous (LDA) ice.

- ▶ The IPES of AIMD water at ambient conditions contains the signature of ice polymorphism³.

Water at deeply undercooled conditions

- ▶ Deeply undercooled water may hold the clue to understanding water anomalies; it is metastable and it is important to understand how crystallization occurs.
- ▶ Dynamics at deeply undercooled conditions is very sluggish and not accessible to *ab initio* simulations: coarse grained models are essential.

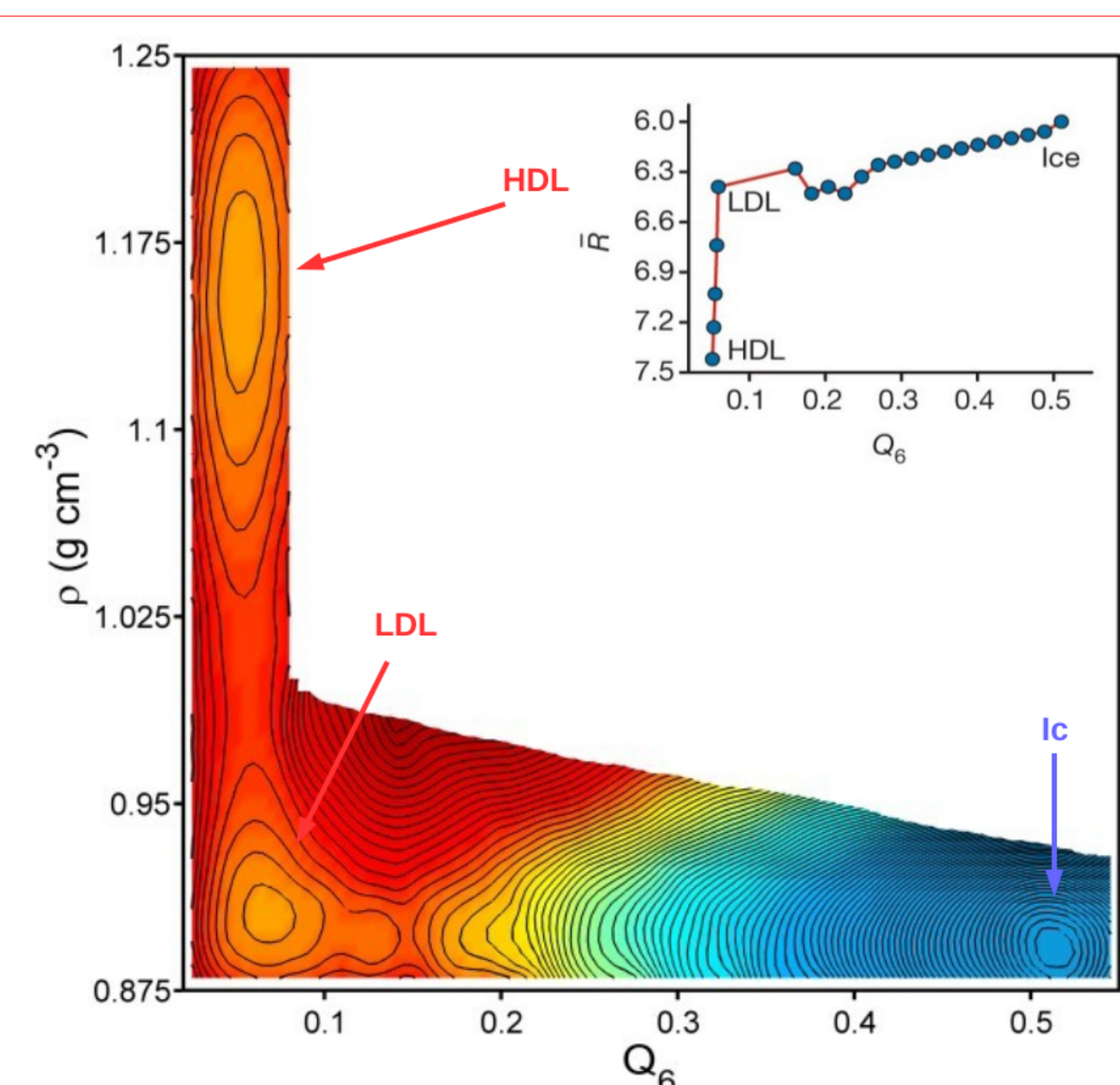


Figure 2 : Free energy plotted vs density and global order parameter Q_6 . Simulations used 192 molecules at $T = 228.6$ K and $p = 2.2$ kbar. Q_6 measures angular order. Inset: the average ring length \bar{R} as a function of Q_6 .

- ▶ Monte Carlo simulations with enhanced sampling techniques show the existence of three basins in the free energy landscape of deeply supercooled ST2 water: a high density liquid (HDL) basin, a low density liquid (LDL) basin, and a stable cubic ice (Ic) basin⁴. The H-bond network shows a distinct topology, measured by the ring distribution, in each of these three basins.
- ▶ The non monotonic behaviour of \bar{R} between LDL and Ic (inset) suggests a complex rearrangement of the H-bond network during crystallization.

A new order parameter to characterize local environments

- ▶ We introduce the local order parameter⁵ $Q = q \otimes Q_{12}$ as the product of the tetrahedral⁶ q for the first 4 neighbors of a given site and of the Steinhardt⁷ Q_{12} restricted to the 12 next neighbors.

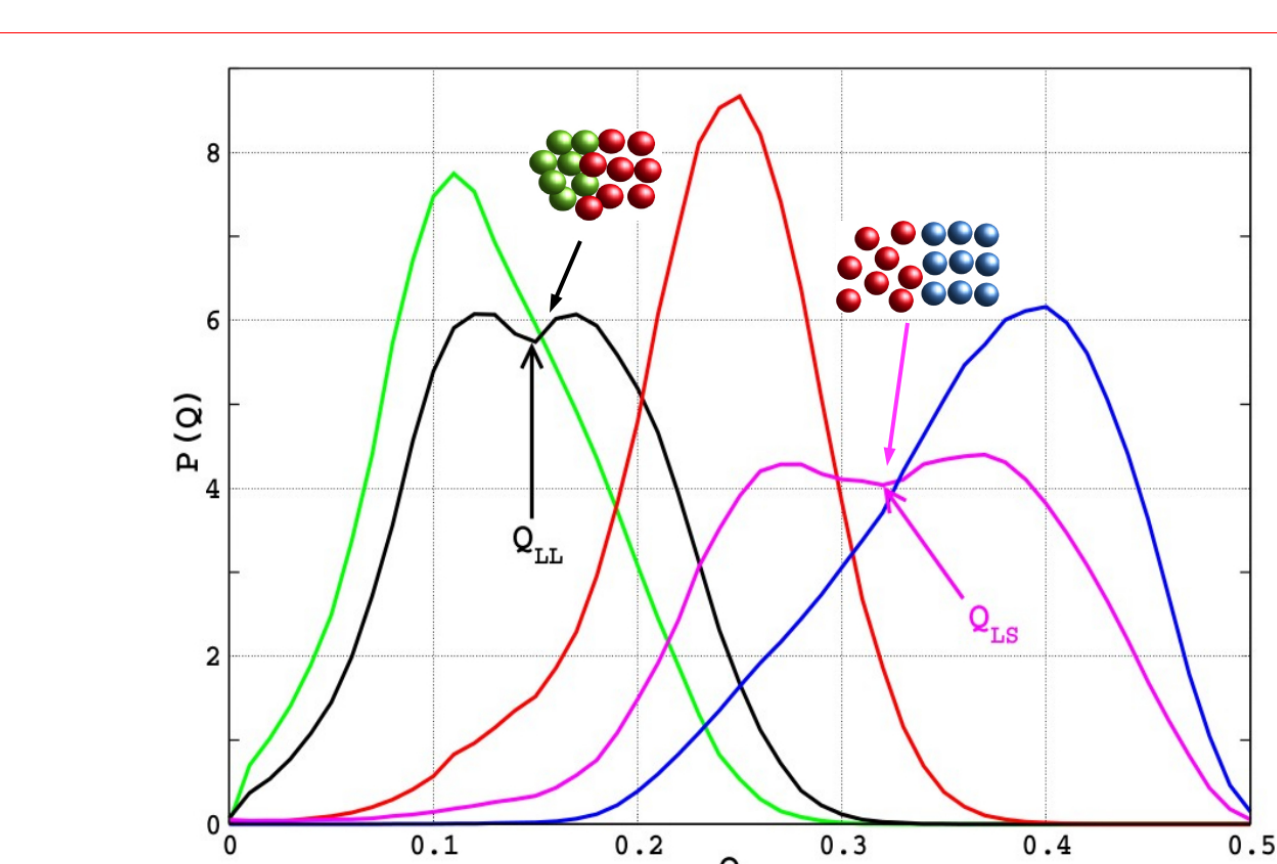


Figure 3 : Distribution of Q in the HDL (green), LDL (red) and Ic (blue) basins. Black and violet curves are bimodal distributions and the two minima define isosbestic points Q_{LL} and Q_{LS} .

- ▶ In the two transition regions (HDL-LDL and LDL-Ic) the Q distribution is bimodal.
- ▶ Ice I can crystallize in cubic (Ic) or hexagonal (Ih) forms. Q does not distinguish Ic from Ih. For that we use the Steinhardt W_4 order parameter⁸ associated to the first 16 nearest neighbors, whenever a site has $Q \geq Q_{LS}$.

Spontaneous crystallization in MD simulation

- ▶ We performed MD simulations at $T = 235$ K for 2500 ST2 molecules⁵ in a parallelepipedal box with fixed volume corresponding to a density ρ of 0.98 g cm⁻³.

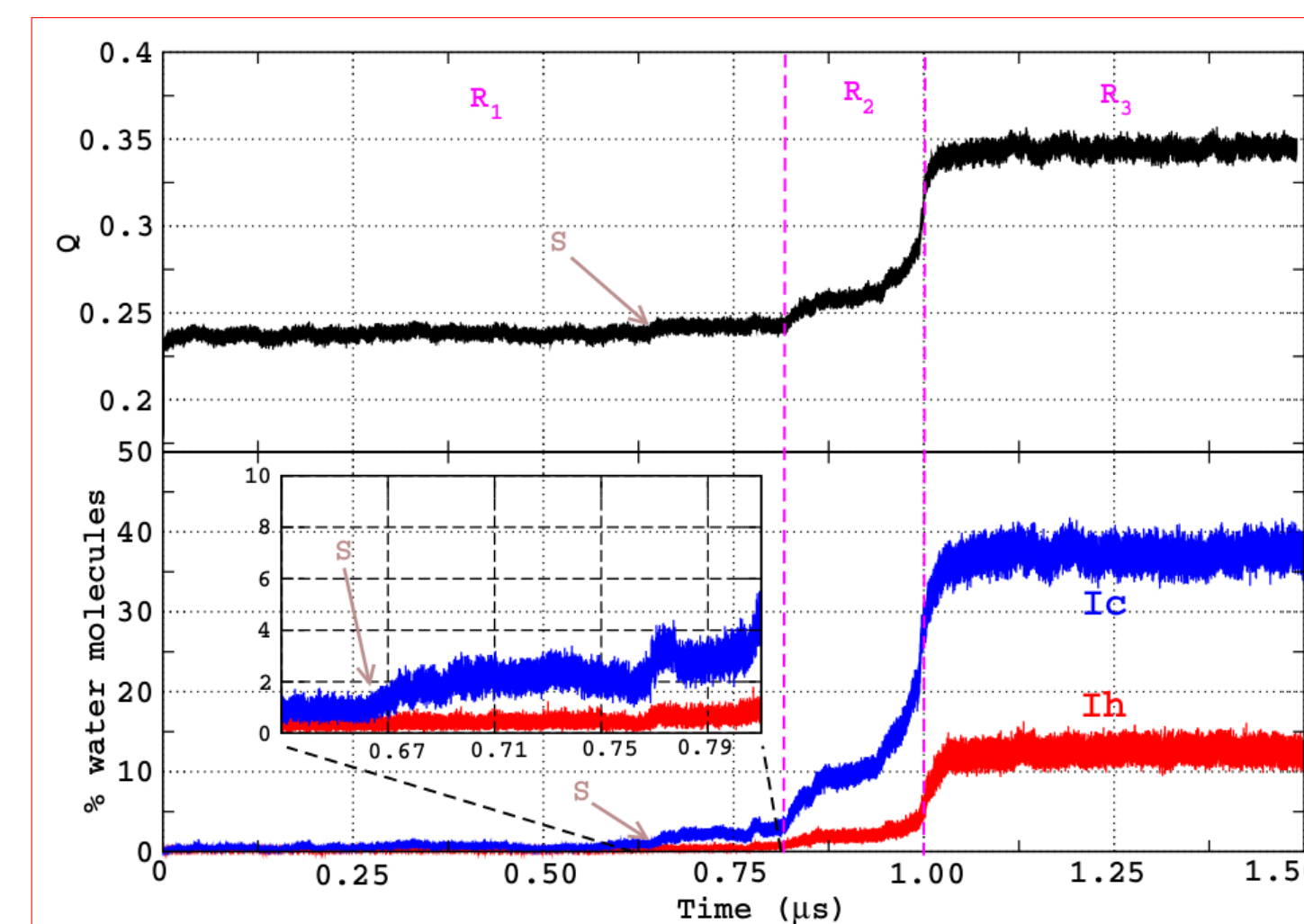


Figure 4 : Time evolution of Q (black line) in an MD trajectory lasting $1.5 \mu s$. The blue and the red lines give the fraction of Ic and Ih sites, as identified by W_4 .

- ▶ The three regions R_1 , R_2 , R_3 correspond respectively to the supercooled liquid, the formation and growth of the first sizeable crystalline seed, and the completed nucleation of ice.
- ▶ Ic and Ih sites keep appearing and disappearing randomly during the first 600 ns of simulation. The small shoulder S at around 670 ns marks a small but discernable jump in the fraction of Ic sites.

- ▶ The final ice structure contains a predominant Ic region separated by a grain boundary from a Ih region. Ic is the stable form of ST2 ice at this thermodynamic condition.

Euclidean structures in the molecular arrangement

- ▶ The tetrahedrality of the first shell of neighbors (4) is not sufficient to distinguish LDL and ice (which have same q). The second shell of neighbors (12) is disordered in LDL and ordered in ice.

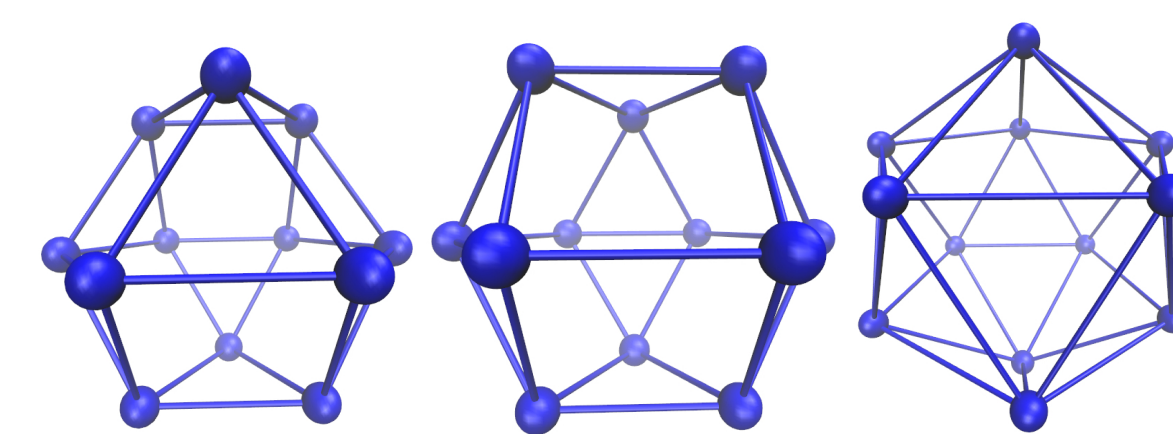


Figure 5 : Schematic representation: the cuboctahedron (left panel), the anticuboctahedron (middle panel) and the icosahedron (right panel).

- ▶ Three ordered Euclidean structures are possible with 12 sites: the cuboctahedron, the anticuboctahedron and the icosahedron. Only the cuboctahedron and the anticuboctahedron are compatible with a tetrahedral first shell.

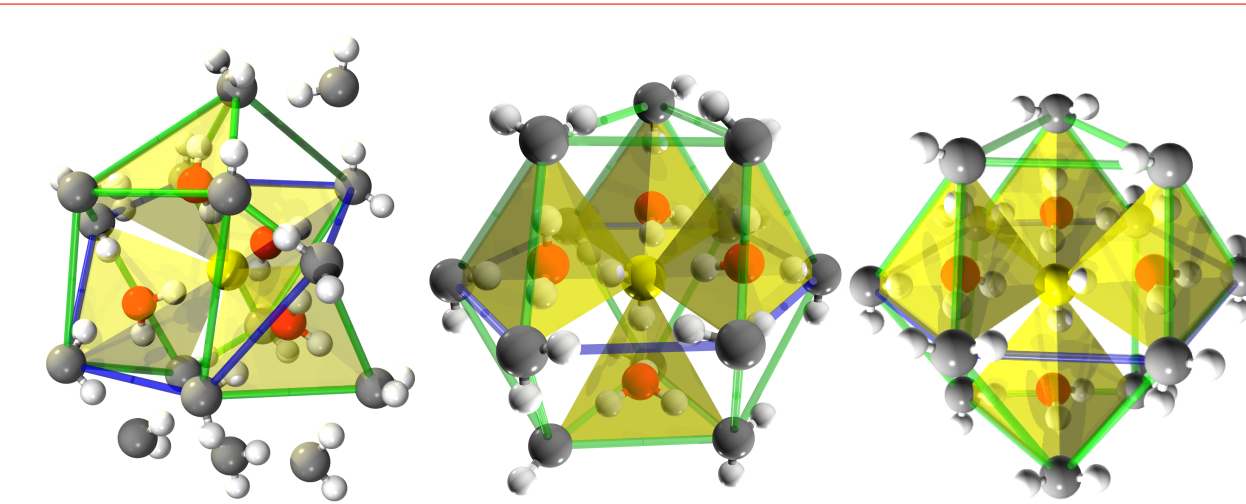


Figure 6 : A site (yellow molecule) with its first 16 nearest neighbors in a snapshot of LDL (left), Ih (center) and Ic (right). The yellow shaded regions indicate tetrahedra that share the central site as a vertex.

- ▶ In LDL, the 4 tetrahedra are free to rotate around the shared vertex, while in Ic and in Ih they are ordered and fixed.
- ▶ In LDL, the possibility for the four tetrahedra to rotate around the shared vertex, can generate only Ic and Ih as stable structures.

References and Acknowledgments

1. Stillinger, F. H., and Weber, T. A., *Science*, **225**, 983, (1984)
 2. Shiratani, E., and Sasai, M., *J. Chem. Phys.*, **104**, 7671 (1996)
 3. Santra, B., DiStasio R. A. Jr., Martelli, F., and Car, R., *Mol. Phys.*, doi:10.1080/00268976.2015.1058432
 4. Palmer, J. C., Martelli, F. Liu, Y. Car, R. Panagiotopoulos, A. Z. and Debenedetti, P. G., *Nature*, **510**, 385-388 (2014)
 5. Martelli, F., Palmer, J. C., Singh, R., Debenedetti, P. G., and Car, R., In preparation
 6. Errington, J. R. and Debenedetti, P. G., *Nature*, **409**, 318 (2001)
 7. Steinhardt, P. J., Nelson, D. R., and Ronchetti, M., *Phys. Rev. B*, **28**, 2, (1983)
 8. Steinhardt, P. J., Nelson, D. R., and Ronchetti, M., *Phys. Rev. Lett.*, **47**, 18, (1981)
- We thank support from the SciDAC program through the DOE under Grant No. DE-SC0008626. This research used resources of the NERSC, a DOE Office of Science User Facility supported by the Office of Science of the U.S. Department of Energy under Contract No. DE-AC02-05CH11231